

Ferromagnetic Resonance in Metals. Frequency Dependence

ZDENEK FRAIT* AND HAROLD MACFADEN

Department of Physics, University of North Carolina, Chapel Hill, North Carolina

(Received 29 March 1965)

The FMR (ferromagnetic-resonance) measurements were performed in single crystals of silicon-iron, nickel-iron, nickel, and hcp cobalt in the frequency region 8–140 Gc/sec at room temperature. The samples, in the form of thin discs, were statically magnetized parallel to the plane of the disc. Their thickness was at least one order of magnitude greater than the penetration depth at microwave frequencies. The values of linewidths, magnetocrystalline anisotropy constants, and g factors were obtained. A macroscopic theory of the resonance line shape was developed, including simultaneously the effects of skin penetration of microwave field, the pinning conditions of the surface spins, and the relaxation damping in the Landau-Lifshitz form. The linewidth frequency dependence of the materials with small values of magnetocrystalline and magnetostriction constants (silicon-iron and nickel-iron) can be fairly well explained assuming a small amount of surface spin pinning and a certain value of the frequency-independent Landau-Lifshitz damping constant. The possible origin of pinning and damping is discussed. The linewidths of highly magnetostrictive and anisotropic materials (cobalt and nickel) suggest a large inhomogeneous broadening, probably due to imperfections and inhomogeneities in crystal structure of the samples. The values of magnetocrystalline anisotropy constants agree mostly with the results of static measurements. The values of g factors were found independent of frequency and in good agreement with the Kittel-Van Vleck theory.

INTRODUCTION

IT has been known, since the work of Rado and Weertman,¹ that in some bulk ferromagnetic metals² the ferromagnetic-resonance (FMR) linewidth measured in the centimeter-wavelength region can be only a few tens of oersteds. Until that time the experimental linewidths in poly- or monocrystalline metals were measured around several hundred oersteds. Later on, narrow FMR linewidths were obtained on whisker-type single crystals of iron³ and fcc cobalt,⁴ on bulk single crystals of silicon-iron and permalloy,⁵ and on nickel single-crystal whiskers and platelets.⁶ In all these experiments the values of the spectroscopic splitting factor (g factor) were in reasonable agreement with the measurements of the gyromagnetic factors (g' factor) and the Kittel-Van Vleck theory.⁷ The major part of observed linewidths was explained by the penetration-depth exchange broadening⁸ (see next paragraph). Some authors assumed an additional linewidth-broadening mechanism caused by surface spin pinning⁵ or by relaxation damping.⁶

To put more light onto the mechanism of linewidth broadening in ferromagnetic bulk metals, we have

performed low-power FMR measurements in single crystals of silicon-iron, nickel-iron, nickel, and hcp cobalt. We have chosen to vary the microwave frequency in order to investigate changes in the linewidths, because in such an experiment the static properties of the sample (saturation magnetization, electrical resistivity, surface properties⁹) remain constant. Varying the linewidth by changing the temperature of the sample means also the simultaneous change of all these static properties, and the analysis of the data is more complicated. The frequency interval of our FMR experiments was from 9 to 140 Gc/sec; the samples were measured at room temperature only.

The present work is described in detail in several sections. Firstly, the more elaborate macroscopic theory of FMR in bulk metals is presented. A section describing the preparation of the samples and the experimental equipment follows. Finally, the results of frequency-dependence measurement of linewidth, magnetocrystalline anisotropy constants, and g factor are described and compared with the theory. The possible physical origins of the linewidth-broadening mechanisms are briefly discussed.

I. THEORY

In the FMR experiments in bulk metals an inhomogeneous high-frequency magnetization always exists because of limited penetration of the electromagnetic field into the material. Kittel and Herring¹⁰ and MacDonald¹¹ pointed out the possible influence of this effect on the resonance line shapes. The exact theory of FMR in metals was developed by Ament and Rado.⁷ They were studying the case of parallel configuration

* On leave from Institute of Physics, Czechoslovak Academy of Sciences, Prague.

¹ G. T. Rado and J. R. Weertman, *Phys. Rev.* **94**, 1386 (1954).

² By the term "bulk" we describe samples whose dimensions are several times larger than the penetration depth of the microwave frequency used in the FMR experiments.

³ D. S. Rodbell, *J. Appl. Phys.* **30**, 187S (1959); see also *Growth and Perfection of Crystals*, edited by C. A. Neugebauer, J. B. Newkirk and D. A. Vermilyea (John Wiley & Sons, Inc., New York, 1958), p. 247.

⁴ Z. Frait, *Czechoslov. J. Phys.* **B10**, 546 (1960).

⁵ Z. Frait, B. Heinrich, and M. Ondris, *Phys. Letters* **3**, 276 (1963); Z. Frait and B. Heinrich, *J. Appl. Phys.* **35**, 904 (1964).

⁶ D. S. Rodbell, *Phys. Rev. Letters* **13**, 471 (1964); and to be published.

⁷ C. Kittel, *Phys. Rev.* **76**, 743 (1949); J. H. Van Vleck, *ibid.* **78**, 266 (1950).

⁸ W. S. Ament and G. T. Rado, *Phys. Rev.* **97**, 1558 (1954).

⁹ By "static surface properties" we mean, e.g., the existence of a surface oxide layer, the decrease of spontaneous magnetization at the surface.

¹⁰ C. Kittel and C. Herring, *Phys. Rev.* **81**, 861 (1951).

¹¹ J. R. MacDonald, *Proc. Phys. Soc. (London)* **64**, 968 (1951).

(the direction of the static magnetization parallel to the sample surface),¹² assuming a nonzero relaxation damping in the Landau-Lifshitz (L.L.) form¹³ and free motion of the magnetization vector at the sample surface. Their exact final formulas are complicated and can be evaluated for a given material and frequency only by using a computer; for sufficiently low frequencies they obtained simple analytic formulas. Later on MacDonald¹⁴ published a similar theory, but for an arbitrary thickness of sample; at low frequencies for bulk metals he obtains the Ament-Rado formulas. Other approximative formulas suitable for use at low frequencies were given by Rado and Weertman¹⁵ (also for the case of completely pinned magnetization vector at the sample surface), by Seavey,¹⁶ Kaganov and Lu¹⁷ and Frait (for the case of partially pinned surface magnetization).¹⁸

In our experiments some frequencies used were well above the limit where low-frequency approximation of the theory can be used; moreover, evidence of a certain amount of surface magnetization pinning was noticed. Therefore, we had to evaluate new exact formulas by means of which the experimental and theoretical results can be compared. The method of solving the problem is in principle the same as in the work by Ament and Rado,⁷ but introducing more general boundary conditions makes the theory more complicated. Here we shall present the main outline of the calculations, for more details and comments regarding the method see Refs. 7, 14, 15. As all of our linewidth measurements were performed with static magnetic field along the easy axis of magnetocrystalline anisotropy, the effect of anisotropy and sample demagnetization can be simply described by adding the values of the effective anisotropy field, demagnetizing field, and external static field, with proper signs.¹⁹ Where not stated otherwise, Gaussian units were used.

First the case of propagation of electromagnetic linearly polarized high-frequency field in the metal ferromagnet is to be solved. The ferromagnetic material is statically magnetized to the value M_s (saturation magnetization) along the z axis. The internal static magnetic field H_z , which is the sum of external, demagnetizing, and effective anisotropy field, lies in the plane of the sample. The microwave field with the frequency ω is propagating in the sample along the y axis with its magnetic component perpendicular to the H_z direction.

As we are interested in FMR performed at low microwave powers only, we assume that the high-frequency components of the electromagnetic field and magnetization are much smaller than H_z and M_s . Using the Maxwell equations and Landau-Lifshitz equation¹³ for the motion of the magnetization vector \mathbf{M} in the form

$$\partial\mathbf{M}/\partial t = \gamma(\mathbf{M} \times \mathbf{H}) + (2A\gamma/M_s^2)(\mathbf{M} \times \nabla^2\mathbf{M}) - (\lambda/M_s^2)[\mathbf{M} \times (\mathbf{M} \times \mathbf{H})], \quad (1)$$

we obtain a secular equation for the propagation constants K of the microwave field:

$$K^6 - c_1K^4 + c_2K^2 - c_3 = 0, \quad (2)$$

where

$$\begin{aligned} c_1 &= 1 + 2\eta + i2E\Omega, \\ c_2 &= (\eta + \eta^2)(1 + L^2) - \Omega^2 \\ &\quad + i[\Omega L(1 + 2\eta) + 4E\Omega(1 + \eta)], \quad (3) \\ c_3 &= -4E\Omega^2(1 + \eta)L + i2E\Omega[(1 + \eta)^2(1 + L^2) - \Omega^2]. \end{aligned}$$

The following abbreviations are used:

$$\begin{aligned} \Omega &= \omega/(\gamma 4\pi M_s), \quad \eta = H_z/(4\pi M_s), \\ L &= \lambda/(M_s \gamma), \quad E = 4\pi \times 10^{-3} \times A\gamma/(M_s \rho), \\ K &= (k/M_s)(A/2\pi)^{1/2}. \quad (4) \end{aligned}$$

Here $\gamma = g\mu_B\hbar^{-1}$ is the spectroscopic splitting ratio, g the spectroscopic splitting factor (g factor), μ_B the Bohr magneton, \hbar Planck's constant divided by 2π , A the exchange constant [in the localized-spin model of ferromagnet $A = a^2IM_s^2/(N\mu_B^2g^2)$, with the a -lattice constant, I the exchange integral, and N the number of atoms per unit volume], λ the phenomenological L.L. damping constant, and ρ the resistivity (in microhm cm).

In our experiments the FMR absorption is proportional to the change of the real part of the surface impedance of thin ferromagnetic discs (see Sec. II). The surface impedance Z is defined²⁰ as the ratio of the tangential components of electric and magnetic microwave fields (denoted by e_z and h_x , respectively) at the surface of the material ($y=0$). In the following we shall use an effective surface impedance⁷ Z' :

$$Z' = (2\pi A)^{1/2}(\rho M)^{-1} 2c \times 10^{-3} (e_z/h_x)_{y=0}. \quad (5)$$

To evaluate the components of the electromagnetic field at the surface and to combine the surface impedance with the results of the theory we have to introduce boundary conditions into the computation. There are three waves propagating into the metal [which are determined by the three positive solutions of propagation constants by Eq. (2)]; therefore we need four conditions for calculating Z' and the amplitudes of the three waves. Two of them are the continuity require-

¹² In this paper, we are concerned with the FMR only in the parallel configuration.

¹³ L. Landau and E. Lifshitz, *Physik. Z. Sowjetunion* **8**, 153 (1935).

¹⁴ J. R. MacDonald, *Phys. Rev.* **103**, 280 (1956).

¹⁵ G. T. Rado and J. R. Weertman, *J. Phys. Chem. Solids* **11**, 315 (1959).

¹⁶ M. H. Seavey, Jr., Technical Report No. 239, Lincoln Laboratory, MIT, 1961 (unpublished).

¹⁷ M. I. Kaganov and J. Lu, *Izvest. Akad. Nauk SSSR, Ser. Fiz.* **25**, 1375 (1961).

¹⁸ Z. Frait, *Czechoslov. J. Phys.* **B13**, 535 (1963).

¹⁹ J. O. Artman, *Phys. Rev.* **105**, 74 (1957).

²⁰ A. R. Bronwell and R. E. Beam, *Theory and Application of Microwaves* (McGraw-Hill Book Company, Inc., New York, 1947), Chap. 14.

ments for h_x and e_z components, which yield

$$\sum_{n=1}^3 h_{xn} = h_{x0}, \quad (6)$$

$$\sum_{n=1}^3 K_n h_{xn} = Z' h_{x0}. \quad (7)$$

h_{x0} denotes the value of tangential magnetic component of the microwave field at the air side of the sample-air boundary. In (8) Maxwell's equations and formula (5) were used for expressing components e_{zn} as functions of h_{xn} .

The other two boundary conditions are needed for determination of the ratios of amplitudes of the three waves. These amplitude ratios are determined by the motion of the magnetization vector at the sample surface. The microwave components of magnetization (m_x, m_y) are connected with h_{xn} by the following expressions [obtained from (1) using Maxwell's equations]:

$$m_x = \sum_{n=1}^3 (K_n^2 - 2iE\Omega)(8i\pi E\Omega)^{-1} h_{xn}, \quad (8)$$

$$m_y = \sum_{n=1}^3 (i\Omega + L\eta + L)^{-1} \{ [(K_n^2 - \eta)(K_n^2 - 2iE\Omega) / (8i\pi E\Omega)] + 1/(4\pi) \} h_{xn}. \quad (9)$$

Néel²¹ first mentioned that the symmetry differences among the atoms inside the material and at the surface may influence the resonance absorption in ferromagnets. He has shown that because of these symmetry differences a "surface anisotropy energy" may exist at the surface. Later on Meiklejohn and Bean²² showed that a layer of another ferro- or antiferromagnet at the sample surface may be another cause for the surface anisotropy energy. Rado and Weertman¹⁵ have analyzed in detail how an additional torque acting on the surface atomic magnetic moments due to the existence of surface anisotropy energy will influence the boundary conditions for m_x and m_y at the sample surface. They have obtained, for the case that the surface anisotropy energy is uniaxial with the easy axis parallel to the static magnetization, the equations

$$\partial m_{x,y} / \partial n - (K_s/A) m_{x,y} = 0, \quad (10)$$

and for the case which the easy direction of uniaxial surface anisotropy is normal to the sample surface,

$$\partial m_x / \partial n = 0, \quad \partial m_y / \partial n - (K_s/A) = 0, \quad (11)$$

where $\partial/\partial n$ denotes the derivative in the direction of the surface normal, K_s is the surface anisotropy constant related to the surface anisotropy energy $E_{SA} = K_s \sin^2\phi$

(ϕ is the angle between the static magnetization vector and the easy direction of anisotropy). Soohoo²³ obtained the same conditions by another method.

In our work we shall take both situations, represented by Eqs. (10) and (11), into account. We shall denote the first case by "parallel anisotropy," the second by "perpendicular anisotropy." For the parallel anisotropy case we obtain from Eqs. (8), (9), and (10) the boundary conditions in the form (more approximate conditions for this case were derived by Kaganov and Lu¹⁷)

$$\sum_{n=1}^3 (K_n^2 - 2iE\Omega)(K_n + \xi') h_{xn} = 0, \quad (12)$$

$$\sum_{n=1}^3 [(K_n^2 - 2iE\Omega)(K_n^2 - \eta) + 2iE\Omega] \times (K_n + \xi') h_{xn} = 0, \quad (13)$$

where ξ' denotes the relative surface anisotropy, $\xi' = K_s' M^{-1} (2\pi A)^{1/2}$. We shall use a prime with ξ and K_s in the parallel anisotropy case, two primes in the perpendicular case. Equations (8), (9), and (10) yield for the perpendicular case

$$\sum_{n=1}^3 (K_n^2 - 2iE\Omega) K_n h_{xn} = 0, \quad (14)$$

$$\sum_{n=1}^3 [(K_n^2 - 2iE\Omega)(K_n^2 - \eta) + 2iE\Omega] \times (K_n + \xi'') h_{xn} = 0. \quad (15)$$

Because the surface impedance is obtained by solving the secular equation of the system of Eqs. (8), (9), (12), (13) or (8), (9), (14), (15), we can theoretically compute the surface impedance for every set of resonance parameters η, Ω, E, L, ξ , knowing the solutions of Eq. (2). First we tried to solve Eq. (2) numerically by the direct method¹⁴ (for the resonance parameters given for our experiments). This method was successful at low Ω , but for high frequencies the round-off errors accumulated in the computer at each step of the calculation made the result inaccurate. Therefore we have used the relations

$$Q^2 = c_1 + 2P, \quad P^2 = c_2 + 2c_3^{1/2}Q, \quad R = c_3^{1/2}, \quad (16)$$

where the real part of the quantity $c_3^{1/2}$ is taken as positive and the quantities P, Q, R are given by

$$\begin{aligned} P &= K_1 K_2 + K_1 K_3 + K_2 K_3, \\ Q &= K_1 + K_2 + K_3, \\ R &= K_1 K_2 K_3. \end{aligned} \quad (17)$$

K_1, K_2, K_3 are the solutions of Eq. (2), corresponding to the electromagnetic waves propagating along the $+y$ direction. Using relations (18) we have transcribed the formula for the surface impedance

$$Z = f(K_1, K_2, K_3, \eta, \Omega, E, \xi, L) \quad \text{to} \quad Z = f(P, Q, R, \eta, \Omega, E, \xi, L).$$

²¹ L. Néel, J. Phys. Radium **15**, 225 (1954).

²² W. H. Meiklejohn and C. P. Bean, Phys. Rev. **105**, 904 (1957); W. H. Meiklejohn, J. Appl. Phys. **32**, 1328 S (1962).

²³ R. F. Soohoo, Phys. Rev. **131**, 594 (1963).

It was found that the method of successive approximations for the coupled equations (16), written in the form $P_{n+1} = (\frac{1}{2})(Q_n^2 - c_1)$ and $Q_{n+1} = (\frac{1}{2}R)(P_{n+1}^2 - c_2)$ led to a rapidly divergent sequence of complex numbers, for the range of parameters used. However, when the same method was used with the equations written in the form $Q_{n+1} = (c_1 + 2P_n)^{1/2}$ and $P_{n+1} = (c_2 + 2RQ_{n+1})^{1/2}$, there was convergence within five or six iterations.

After lengthy calculations we have obtained the formulas for the surface impedance (for the method used see Ref. 8, Sec. IV):

$$Z' = \{R[QP - R + \xi'(2P + \xi'Q + 2\eta + 4iE\Omega + 1)] + 2iE\Omega[2\xi'(1 + \eta)Q + \xi'^2(P + 2 + 2\eta)] \times \{R[P + 1 + 2\eta - \xi'^2 + 2\xi'Q] + P\xi'[1 + 2\eta + Q\xi'] + (Q + \xi')[c_2 - 4iE\Omega(1 + \eta)] + \xi'c_2\}^{-1} \quad (18)$$

for the parallel case, and

$$Z' = \{R[QP - R + \xi''(P + \eta + 2iE\Omega)] + 2iE\Omega\xi''(1 + \eta)\Omega \times \{R[P + 1 + 2\eta + Q\xi''] + (Q + \xi'')c_2 - 2iE\Omega(1 + \eta)(\xi'' + 2Q) + P\xi''\eta\}^{-1} \quad (19)$$

for the perpendicular anisotropy case. These formulas can be practically evaluated only by means of a computer. The complete program for obtaining the real and imaginary part of Z' included the solution of Eqs. (16) as described previously and evaluation of formulas (18) and (19) (the program was written in the GAT language and Univac 1105 was used). For fixed values of Ω , E , L , ξ a table of $\text{Re}(Z')$ values was computed for a given set of η values. Using this table an absorption resonance line was plotted, from which the exact value of the relative resonance field η_r and relative linewidth $\Delta\eta$ were obtained. The FMR linewidth ΔH ($\Delta H = 4\pi M_s \Delta\eta$) is the difference between the static magnetic field values, which are read at $1/\sqrt{2}$ of the maximum value of $\text{Re}(Z')$.

To show the character of $\Delta\eta$ frequency dependence we have computed the relative linewidth values $\Delta\eta$ for some selected values of Ω , E , L , ξ' and ξ'' , the results are shown in Figs. 1, 2, 3. The exact Ament-Rado solution⁷ ($L=0$, $\xi=0$) is plotted in all three figures. We see that at low frequencies, i.e., up to $\Omega < 0.15$, the $\Delta\eta$ frequency dependence in the log-log plot is linear (this is the region where approximate formulas can be used), then it deviates from linearity and becomes linear again at high frequencies ($\Omega \geq 2$). In the parallel anisotropy case but with a zero damping (Fig. 1), the existence of surface anisotropy shifts the frequency dependence curve in the log-log plot toward higher $\Delta\eta$ values, but the character of the dependence (the slope of the curves) remains approximately the same. In the perpendicular anisotropy case with zero damping (Fig. 2) the influence of surface anisotropy is negligible at low frequencies ($\Omega < 0.05$), but very pronounced at high Ω ($\Omega > 2$). Finally, in the case of nonzero damping but with no surface anisotropy (Fig. 3) the damping increases the slope of the $\Delta\eta$ frequency dependence. These conclusions

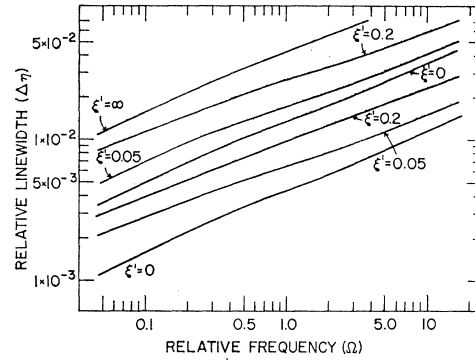


FIG. 1. Theoretically computed frequency dependence of $\Delta\eta$ for the case of parallel surface anisotropy. The lower three curves are computed for $E = 10^{-6}$, the higher four for $E = 10^{-4}$. The curve for $E = 10^{-6}$ and $\xi' = \infty$ practically coincides with the curve for $E = 10^{-4}$ and $\xi' = 0$.

are valid for values of E from 10^{-6} up to 10^{-4} (most of the experimental cases are inside of this interval). Observing the frequency dependence of linewidth in a

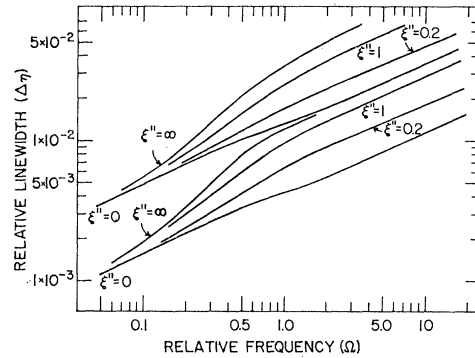


FIG. 2. Theoretically computed frequency dependence of $\Delta\eta$ for the case of perpendicular surface anisotropy ($L=0$). The lower set of curves applies for $E = 10^{-6}$, the higher set for $E = 10^{-4}$.

sufficiently large frequency interval, we can roughly estimate the contributions of various line broadening mechanisms, which are considered in this work. Detailed

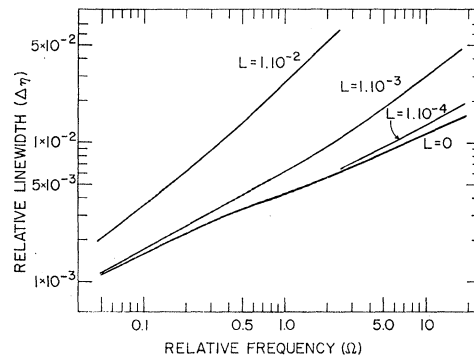


FIG. 3. Theoretically computed frequency dependence of $\Delta\eta$ for the case of nonzero damping ($\xi=0$) and $E = 10^{-5}$.

numerical evaluation of L and ξ values for a given material can be done only by comparing the experimental linewidth values with exact $\Delta\eta$ values computed from the theory.

II. METHOD OF MEASUREMENTS

The single crystals of silicon-iron (3% Si), nickel-iron (58% Ni), pure nickel and hexagonal cobalt were grown by the Bridgman method by Sestak and Tahal.²⁴ The ingots were oriented by means of x rays and cut into thin disks by an electroerosive method using an automatic electric-spark saw built by Libovicky.²⁵ The samples were chemically etched and polished mechanically on both surfaces. Then the samples were annealed in an atmosphere of pure hydrogen for approximately 10 h at elevated temperatures (1000°C for silicon-iron, nickel-iron, and nickel; 380°C for cobalt), and were cooled at the rate of 100°C/h. Finally the samples were electrochemically polished in a solution²⁶ of 80% H_3PO_4 +13% CrO_3 +7% H_2O . Two methods of polishing were used: a "fast" method, in which the density of the polishing current reaches up to 1 A/cm² and the polishing is finished in tens of seconds,²⁷ and a "slow" method, designed by Powers,²⁸ which gave better results with respect to waviness of the sample. The final result was a lustrous polish, the maximum angle of deflection of tangential plane to individual points at the surface was about 1.5° (determined by the microscopic observations of the surface). Such small deflection has no influence on the FMR in the parallel configuration of the experiment.²⁹ The final form of the samples was thin disks, with a diameter of about 9.0 mm and thickness from 0.1 to 0.25 mm.

To exclude the possible influence of internal field inhomogeneities,³⁰ the samples were covered with a thin gold foil (thickness of which was about 10 μ m) except a small area (0.7 mm diameter) at the center of the sample. The static demagnetizing factors of the samples N were computed from the Maxwell's formula $N \approx \pi^2(a/b)$, where a and b are the thickness and diameter, respectively. Several waveguide setups were used in the experiments. The microwave energy was generated by low-power (up to 100-mW) klystrons in the frequency region 8 to 72 Gc/sec. The measurements at 105 Gc/sec were performed at the third-harmonic frequency from a crystal multiplier using a high-power 8-mm klystron; in the waveband of 140 Gc/sec a second-harmonic frequency from a crystal multiplier and a 4-mm klystron was used. The power from the klystron

or harmonic generator was monitored by a silicon diode via a directional coupler and guided through a ferrite isolator and attenuator to a straight rectangular waveguide section. The sample was placed at the end of this section forming a short, the energy reflected from the sample was separated by a directional coupler, by a hybrid ring, or by a magic tee, depending on the waveband, and detected by a semiconductor diode. The monitor line was equipped with a calibrated resonator, by means of which the microwave frequency was measured with an accuracy to 1×10^{-4} .

The static magnetic field was generated by a 9-in. 60-kW electromagnet, the current of which was electronically stabilized. For the high-field measurements (up to 42 kOe), tapered iron-cobalt pole pieces and a gap of 9 mm were used. The static magnetic field was measured by a rotating coil gaussmeter, which was calibrated by means of H_2O and D_2O nuclear magnetic resonance. The output of the gaussmeter was fed to the x axis of an X - Y recorder.

On the back side of the sample a loop of copper wire (diameter 0.8 mm) was placed. A current of 102 kc/sec was passed through this wire and the stray magnetic field of the loop modulated the static magnetic field in the sample.³¹ The microwave signal reflected from the sample was modulated by the 102-kc/sec frequency when ferromagnetic resonance occurred; the 102-kc/sec signal was proportional to the derivative of the microwave absorption in the sample versus the static magnetic field. This signal, detected by the diode, was amplified by a selective amplifier (with a tuned input circuit³² and electromechanical selective filter) and detected by a lock-in detector. The lock-in output was fed to the Y axis of the X - Y recorder.

The advantage of the detection method using auxiliary modulation of the static magnetic field lies in the high sensitivity of the apparatus, which enables observation of FMR at a small sample region without the use of resonant cavities (no frequency stabilization of the microwave source is needed). The disadvantage of this method is that the derivative of the microwave absorption does not give complete information about the real part of the surface impedance Z' . In our experiments we are observing the quantity (102-kc/sec voltage at the detection diode) which is proportional to the derivative of the change of $Re(Z')$ due to the FMR effect only [this part of $Re(Z')$ we denote by $Re(Z')_{FMR}$]. The constant part of $Re(Z')$, which is due to the eddy-current losses in the metal [denoted by $Re(Z')_{\infty}$ —the FMR effect vanishes at very high values of η], cannot be detected in our case. Therefore the following process was used in comparing theoretical and experimental results. First, observing the character of the experi-

²⁴ From the Department of the Mechanical Properties of Solids, Institute of Physics, Prague.

²⁵ S. Libovicky, Czechoslov. J. Phys. **A11**, 493 (1961).

²⁶ B. Sestak, Czechoslov. J. Phys. **B10**, 91 (1960).

²⁷ N. Bloembergen, Phys. Rev. **78**, 572 (1950).

²⁸ R. W. Powers, Electrochem. Technol. **2**, 274 (1964).

²⁹ Z. Frait and M. Ondris, Czechoslov. J. Phys. **B12**, 485 (1962).

³⁰ Z. Frait and B. Heinrich, Bull. Ampere **10**, 1381 S (1961).

³¹ Z. Frait, Czechoslov. J. Phys. **B9**, 403 (1959).

³² W. Gordy, W. V. Smith, and R. F. Trambarulo, *Microwave Spectroscopy* (John Wiley & Sons, Inc., New York, 1953), pp. 60, 61.

mentally observed linewidth frequency dependence, preliminary values of ξ and L were chosen for the computation of the theoretical resonance curves [plots of $\text{Re}(Z')$ versus η]. From $\text{Re}(Z')$ curves the reduced absorption curves [plots of $\text{Re}(Z')_{\text{FMR}}$] are easily computed by the relation $\text{Re}(Z')_{\text{FMR}} = \text{Re}(Z') - \text{Re}(Z')_{\infty}$, where $\text{Re}(Z')_{\infty} = (E\Omega)^{1/2}$ (see Ref. 14). The experimental absorption curves (obtained by graphical or numerical integration from the plots of the derivative of the FMR absorption) were then directly compared with the theoretical $\text{Re}(Z')_{\text{FMR}}$ curves, and ξ and L values were adjusted to get the best agreement of experiment and theory in the whole frequency interval.

III. RESULTS OF EXPERIMENTS. DISCUSSION

A. FMR Linewidths

The FMR measurements were performed on crystallographically oriented single crystals of each material. The face of the samples was parallel to the crystallographic planes (010), (010), (111), (100) for silicon-iron, nickel-iron, nickel, and hcp cobalt, respectively. The direction of the external static magnetic field was along the easy direction of magnetocrystalline anisotropy. The results of linewidth measurements for two samples of silicon-iron are plotted on Fig. 4 as circles. The difference in linewidth values for both samples at the same frequency was 3%; the low signal-to-noise ratio in measurements at very high frequencies (about 100 Gc/sec) lowered the accuracy of linewidth measurements to approximately 10%. First we tried to fit the experimental curves with one of the parameters ξ or L , but with no success. The best agreement was obtained with $L = 1.4 \times 10^{-3}$ (L.L. damping constant $\lambda = 4.1 \times 10^7$ radians/sec) and with $\xi' = 0.01$ (parallel surface anisotropy $K_s' = 0.056$ erg/cm²). The following values of static parameters were used: $4\pi M_s = 20\,240$ emu,³³ $\rho = 47$ microhm cm,³³ $A = 1.9 \times 10^{-6}$ erg/cm.³⁴ The agreement in the line shape between theory and experiment was relatively good (see Fig. 5).

Similar results were obtained measuring linewidths on three samples of nickel-iron single crystal (Fig. 6). The

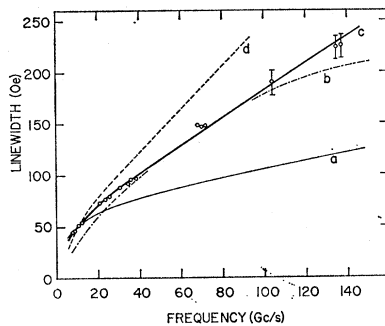


FIG. 4. The results of linewidth measurements for silicon-iron (points denoted by circles) and linewidth frequency dependence, computed from theory. (a) $\xi' = 0.03$, $L = 0$; (b) $\xi' = 0.42$, $L = 0$; (c) $\xi' = 0.01$, $L = 1.4 \times 10^{-3}$; (d) $\xi = 0$, $L = 2.6 \times 10^{-3}$.

³³ R. M. Bozorth, *Ferromagnetism* (D. Van Nostrand, Inc., New York, 1951), Chap. 4.

³⁴ Z. Frait and M. Ondris, *Phys. Status Solidi* **2**, K 185 (1962).

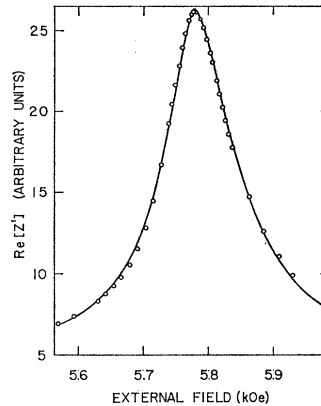


FIG. 5. The shape of FMR absorption line measured (continuous line) and computed from the theory (points denoted by circles) for silicon-iron; the following parameters were used in the theory: $\Omega = 0.608$, $L = 1.4 \times 10^{-3}$, $\xi' = 0.01$.

difference in $\Delta\eta$ values for the three samples was 4% (at the same frequency); at very high frequencies 10%. The best agreement with the theory was obtained using $L = 1.5 \times 10^{-3}$ ($\lambda = 4.2 \times 10^7$ radians/sec) and $\xi' = 0.07$ ($K_s' = 0.2$ erg/cm²). The values of the parameters used in the calculation were $4\pi M_s = 15\,600$ emu,³⁵ $\rho = 26$ microhm cm,³⁵ $A = 1.05 \times 10^{-6}$ erg/cm.³⁶

The values of the surface anisotropy constant K_s , which are used to explain the observed linewidth frequency dependence, agree in order of magnitude with values reported previously⁵ and with the theoretical estimates of Néel theory.²¹ An influence of surface conditions on FMR is indicated by the fact that the linewidth of iron-silicon crystals increases if the samples are kept outside the desiccator for a long time. We have observed an increase of ΔH from 46 Oe up to 80 Oe in six months (at 9.2 Gc/sec; in iron-nickel crystals the increase was only approximately 20%). A similar effect was observed by Rodbell in iron single-crystal whiskers.³ The value $\Delta H = 80$ Oe supports further the assumption that the easy axis of surface anisotropy lies in the sample surface; in the perpendicular case even the infinite value of K_s could not increase the linewidth to 170% of the original value at 9 Gc/sec (see Fig. 2). The origin of the surface anisotropy is not clear: besides the Néel's mechanism,²¹ a surface layer with different value of magnetization (caused probably by partial surface

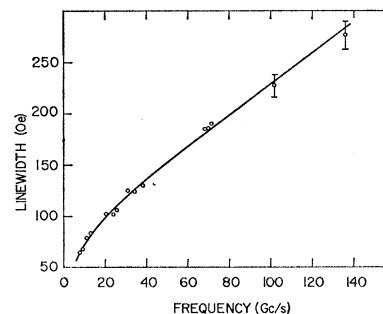


FIG. 6. The results of linewidth measurements for nickel-iron (points denoted by circles) and linewidth frequency dependence, computed from theory ($\xi' = 0.07$, $L = 1.53 \times 10^{-3}$).

³⁵ See Ref. 33, Chap. 5.

³⁶ M. Ondris and Z. Frait, *Czechoslov. J. Phys.* **B11**, 883 (1961).

oxidation) influences the motion of the surface spins^{37,38} (Rado and Weertman detected such a layer of unknown composition on the surface of their nickel-iron samples).¹⁵ The decrease in magnetization value at the surface of a ferromagnet, computed by the atomic-planes sublattice method,^{39,40} can also lead to the same effect. The value of K_s assumed in our work is much smaller than the values needed for explanation of nearly quadratic standing spin-wave spectra in thin film.⁴¹ Probably a transition layer between the film substrate and film causes the large pinning of the surface spin motion.

Let us discuss further the possible origin of the relaxation mechanism which is phenomenologically described by the L.L. damping parameters λ . The direct spin-lattice relaxation process was recognized as being too small to give a contribution to the FMR linewidth.⁴² Three other mechanisms were considered, all of them based on the assumption that the relaxation of the conduction electrons' magnetic moments in the lattice is a very fast process.⁴³ In the first mechanism an s electron flipping its spin from down to up together with the destruction of one spin wave (or an inverse process) is considered.^{43,44} However, the value of L computed from this theory is three orders of magnitude lower than the value measured in our experiments; therefore this process is not effective in the resonance-line broadening. The second relaxation process involves the exchange interaction between the spins of s and d electrons. For such a process Kittel and Mitchell⁴⁵ computed the relaxation time τ , ($1/\tau \approx \omega L$), which is proportional to the square of the s - d exchange integral (I_{sd}). We have computed the values of I_{sd} from that theory using the experimental value of L and the following relations and parameters: κ , the wave vector of the spin waves which are excited by the microwave field in the sample, $\kappa = \delta^{-1} \mu_2^{1/2}$; μ_2 , the imaginary part of effective permeability,⁷ $\mu_2 = \text{Re}[\frac{1}{2}(E\Omega)^{-1}Z'^2]$; Z' , computed from formula (19). As a result, the values of I_{sd} for silicon-iron are obtained as (1.1, 0.8, 0.7, 0.6, 0.6) $\times 10^{-2}$ eV, and for nickel-iron (0.9, 0.8, 0.8, 0.7, 0.6) $\times 10^{-2}$ eV at 9, 25, 36, 72, and 144 Gc/sec, respectively. These values of I_{sd} are one order of magnitude smaller than the values used by

other authors⁴⁶; also such a frequency dependence of I_{sd} is improbable. Moreover Vonsovsky and Izjumov⁴⁷ note that use of more exact treatment of the s - d exchange interaction shows that the energy of a spin wave is too small to scatter a conduction electron in the first order. The second-order process is also negligible.⁴⁸

The third mechanism considers the interaction of ferromagnetic spins with conduction electron current.^{43,44} We have computed the L values from the formula, given by Abrahams,⁴³ using parameters mentioned above, the numbers⁴⁹ of s electrons per atom, 0.1 and 0.2, the values⁵⁰ of Fermi energy, 8.84 and 8.99 eV, for silicon-iron and nickel-iron, respectively. The theoretical values of L for iron are (0.35, 0.69, 0.92, 1.35, 1.6) $\times 10^{-3}$ and for nickel-iron (0.11, 0.28, 0.29, 0.5, 0.5) $\times 10^{-3}$ at 9, 25, 36, 72, and 144 Gc/sec, respectively. These values of L are mostly lower than the experimental ones; their frequency dependence contradicts the experimental results. Abrahams uses in his formula a screening factor, which represents the influence of conduction-electron plasma vibrations. Some authors are opposed to the use of a screening factor at microwave frequencies,^{44,51} but in case this factor is left completely out, the theoretical value of L would be two orders of magnitude larger than it is observed in the experiment. Introducing a phenomenological frequency-dependent screening factor, which will be less effective at lower frequencies and more at higher (in mm-wavelength region) frequencies, would bring the relaxation time caused by this relaxation mechanism into agreement with experiments. We see that none of these theories gives a good agreement with experimental results. Recently Seiden⁵² suggested that the relaxation process is due to two-magnon scattering caused by fluctuations in the pseudodipolar field in the sample. The theory in the present form gives the right order of magnitude of L at lower frequencies, but still does not explain the frequency dependence of linewidth. Frequency-independent values of L of the order 10^{-3} were observed recently in nickel crystals in the form of whiskers and platelets⁵; results of linewidth measurements in pure iron whisker single crystals^{5,53} suggest such L values also. We feel, therefore, that besides a need for more FMR linewidth measurements in a large frequency interval, some new theories of FMR relaxation in metals should be considered.

³⁷ P. E. Wigen, C. F. Kooi, M. R. Shanabarger, V. K. Cummings, and M. E. Baldwin, *J. Appl. Phys.* **34**, 1137 (1963); C. F. Kooi, W. R. Holmquist, and P. E. Wigen, *J. Phys. Soc. Japan* **17**, Suppl. B-I, 599 (1962).

³⁸ P. Wolf, *J. Appl. Phys.* **34**, 1139 (1963); Ph.D. thesis, Johannes Gutenberg University, Mainz, 1963 (unpublished).

³⁹ L. Valenta, *Izvest. Akad. Nauk SSSR, Ser. Fiz.* **21**, 879 (1957); *Phys. Stat. Sol.* **2**, 112 (1962).

⁴⁰ J. J. Pearson, *J. Appl. Phys.* **36**, 1061 (1965).

⁴¹ M. Nisenoff and R. W. Terhune, *J. Appl. Phys.* **36**, 732 (1965); Z. Frait and E. N. Mitchell, *Proc. Phys. Soc. (London)* (to be published.)

⁴² A. Akhieser, *J. Phys. USSR* **10**, 217 (1946); C. Kittel and E. Abrahams, *Rev. Mod. Phys.* **25**, 233 (1953).

⁴³ E. Abrahams, *Phys. Rev.* **98**, 387 (1955).

⁴⁴ E. A. Turov, *Ferromagnitnyj Rezonans* (GIFML, Moscow 1961), edited by S. V. Vonsovskij, Chap. 5.

⁴⁵ C. Kittel and A. H. Mitchell, *Phys. Rev.* **101**, 1611 (1956); A. H. Mitchell, *Phys. Rev.* **105**, 1439 (1957).

⁴⁶ T. Kasuya, *Progr. Theoret. Phys. (Kyoto)* **16**, 58 (1956); A. W. Overhauser and M. B. Stearns, *Phys. Rev. Letters* **13**, 316 (1964).

⁴⁷ S. V. Vonsovskij and I. A. Izjumov, *Fiz. Metal. i Metalloved.* **10**, 321 (1960).

⁴⁸ J. Mathon and D. Fraitova, *Phys. Status Solidi* **8**, K 37 (1965).

⁴⁹ J. M. Ziman, *Electrons and Phonons* (Clarendon Press, Oxford, England, 1960), p. 127.

⁵⁰ L. F. Mattheiss, *Phys. Rev.* **134**, A970 (1964).

⁵¹ H. Hasegawa, *Progr. Theor. Phys. (Kyoto)* **21**, 483 (1959).

⁵² P. E. Seiden, *Phys. Rev. Letters* **14**, 370 (1965).

⁵³ D. S. Rodbell, *Resonance and Relaxation in Metals* (American Society for Metals, 1962), Chap. IV; Z. Frait, *Czechoslov. J. Phys.* **B14**, 205 (1964).

TABLE I. Linewidth frequency dependence for nickel and cobalt.

Frequency (Gc/sec)	8.5	25	36	72	105	140
ΔH , Ni (Oe)	460	520	550	800
ΔH , Co (Oe)	1000	1000	1200

The linewidth measurements in single crystals of nickel (2 samples) and hcp cobalt (2 samples) are given in Table I. The differences in $\Delta\eta$ between the two samples of the same material were about 15%. Measurements in nickel at high frequencies were not performed due to the high field limit of the electromagnet used (≈ 42 kOe); in hcp cobalt the high magnetocrystalline anisotropy prevented the measurements at low frequencies. The frequency dependence of linewidth cannot be explained by the macroscopic theory, even assuming infinite value of surface anisotropy. As both nickel and cobalt have large values of magnetostriction and magnetocrystalline anisotropy constants, we think that the large linewidths are caused by inhomogeneities in crystal structure and stresses inside the specimens. This hypothesis is supported by Rodbell's results in nickel whiskers and platelets.⁶

B. Magnetocrystalline Anisotropy Constants

The values of magnetocrystalline anisotropy constants were computed from the resonance field values measured at various angles (ψ) of static field to the anisotropy easy axis direction using the formulas by Artman.¹⁹ It was assumed that the slight shift of resonance field due to the electric conductivity, relaxation damping, and surface anisotropy is independent of ψ . The results of measurements are summarized in Table II. The accuracy of K_1 measurements is 2% for silicon iron and 5% for nickel (the accuracy of K_2 for nickel is 30%). The value of K_1 in nickel iron was smaller than 8×10^3 erg/cm³. The values of anisotropy constants are practically frequency-independent and in agreement with static and dynamic measurements of other authors^{54,55} (only the sign of K_2 in nickel differs from the sign measured statically⁵⁸). More detailed data for cobalt were given in Ref. 56.

TABLE II. Magnetocrystalline anisotropy constants K_1, K_2 (10^{-3} erg/cm³).

Frequency (Gc/sec)	8.5	25	36	72
Fe-3% Si	340	350	295	340
Ni	-55, -20	...	-50, -20	...
Co hcp	5220, 910

⁵⁴ Reference 33, pp. 563-576.⁵⁵ K. H. Reich, Phys. Rev. **101**, 1647 (1956).⁵⁶ Z. Frait, Brit. J. Appl. Phys. **15**, 993 (1964).

C. g Factors

The g factors were computed from the resonance formula

$$\Omega^2 - \Delta\Omega^2 = \eta_r(\eta_r + 1), \quad (19)$$

where η_r is the value of the relative internal static magnetic field at which the real part of surface impedance Z' reaches a maximum. This formula differs from the original Kittel expression⁵⁷ in the term $\Delta\Omega^2$, which represents the influence of electrical conductivity, relaxation damping and surface anisotropy. Knowing the value of magnetocrystalline anisotropy constants from the measurements described in the previous paragraph, and computing $\Delta\Omega^2$ for the case $\xi=0, L=0$ [from plots of theoretical values of $\text{Re}(Z')$ versus η_r], we were able to evaluate approximate values of g factors. These g values were used in all computations concerning the linewidth, from which the nonzero values of ξ and L were obtained. Using once more Eq. (19), where $\Delta\Omega^2$ was recalculated with nonzero values of ξ and L , final values of g factors were computed and are listed in Table III. Let us mention that the differences between the g factors calculated for zero and nonzero values of ξ and L is very small (of the order 10^{-3} for our experiments); the

TABLE III. Frequency dependence of g factors.

Frequency (Gc/sec)	8.5	25	36	72
Fe-3% Si	2.10	2.10	2.10	2.09
Fe-58% Ni	2.11	2.10	2.11	2.11
Ni	2.20	2.21	2.22	2.22
Co hcp	2.18

difference in using approximative and exact values of g factors in calculating linewidths is negligible.

The accuracy of these measurements is 1% for all materials except nickel at frequencies below 70 Gc/sec, where it was 2% (because of large linewidth value). The measurements of high frequencies ($f > 72$ Gc/sec) were not evaluated, because of the lack of accurate absolute measurements of high static magnetic field; the NMR gaussmeter probe was too large to enter the narrow magnet gap. Only relative values of field (suitable for $\Delta\eta$ measurements) were obtained by means of a rotating coil gaussmeter. The values given in Table III are in good agreement with previous measurements (see, e.g., Ref. 58). They were compared with the values g'' , computed from gyromagnetic factors (g') data using the Kittel-Van Vleck theory.^{8,58} For silicon iron $g=2.10$, $g''=2.09$ (the only available value of g' , for pure iron, was used), for nickel iron $g=2.11$, $g''=2.10$, for hcp cobalt $g=2.18$, $g''=2.17$ and for nickel $g=2.21$, $g''=2.20$. The agreement between g and g'' is very good.

⁵⁷ C. Kittel, Phys. Rev. **71**, 270 (1947).⁵⁸ A. J. P. Meyer and G. Asch, J. Appl. Phys. **32**, 330S (1961).

ACKNOWLEDGMENTS

The authors wish to express their appreciation for the hospitality of the Department of Physics, University of North Carolina (U.N.C.), where the measurements were performed partly under the support of the Advanced Research Projects Agency. We would like to acknowledge the stimulating discussions concerning the theory with D. Fraitova; thanks are also due to C. Ross from the Computation Center, U.N.C., for a valuable sug-

gestion in the solution of the Eqs. (16). C. V. Briscoe and E. N. Mitchell from the Department of Physics, U.N.C., and D. S. Rodbell from the General Electric Research Laboratories made helpful comments concerning the measurements and the manuscript. Further, we are greatly indebted to B. Sestak and Z. Tahal for growing the single crystals and to J. Caslavsky, B. Heinrich, J. Hejduk and M. Simanova, all from the Institute of Physics, Prague, Czechoslovakia, for help with the sample preparation.

Fermi Surfaces of Cr, Mo, and W by the Augmented-Plane-Wave Method*

T. L. LOUCKS

Institute for Atomic Research and Department of Physics, Iowa State University, Ames, Iowa

(Received 16 March 1965)

The Fermi surfaces of chromium, molybdenum, and tungsten were calculated using linear-variation functions consisting of 19 augmented plane waves (APW). The muffin-tin potential was constructed from a superposition of atomic potentials centered on the lattice sites. The atomic orbitals were solutions of the Hartree-Fock-Slater self-consistent field. Constant-energy surfaces throughout the Brillouin zone and the volume contained by each of the regions were determined. The Fermi surface was selected from these energy surfaces by the requirement of equal hole and electron volumes. The density of states at the Fermi energy was determined from the slope of the volume-vs-energy curve. The Fermi surfaces of Mo and W were found to be almost identical and similar to the model postulated by Lomer for the Cr-group metals. The Fermi surface of Cr, however, differs from the other two by the disappearance of the hole pockets around N and a shrinking of the knobs on the electron jack. A quantitative comparison between experimental results and the Fermi surface of Mo is presented.

I. INTRODUCTION

A MODEL for the Fermi surface of the chromium-group metals was proposed in 1962 by Lomer.¹ This model was not the result of *ab initio* electronic-structure calculations for these elements. It was deduced from the energy bands for iron which had been determined theoretically by Wood² using the augmented-plane-wave (APW) method. Also available for consideration at that time was a tight-binding calculation for Cr by Asdente and Friedel³ in which only the d bands were considered. Prior to this, there was work done on W by Manning and Chodorow⁴ using the cellular method.

The Lomer model has met with varying degrees of success in comparisons with experimental results. In the original paper the larger pieces of the surface (holes at H , electrons at Γ) were discussed qualitatively, and the antiferromagnetic state of Cr was considered. In a brief note two years later, Lomer⁵ corrected the model such that it was consistent with the requirements im-

posed by crystal symmetry. Here again the qualitative features of the larger pieces of the surface were discussed.

In 1963 Brandt and Rayne⁶ reported de Haas-van Alphen data for the three metals. However, these frequencies corresponded to very small pieces of the surface not well defined in the model (holes at N and either electrons or hole pockets along ΓH). Nevertheless, it was observed that the results for Mo and W were quite similar to each other and different from those for Cr. Further low-field measurements on W by Sparlin and Marcus^{7,8} have been interpreted by these authors as suggesting that the electron surface at Γ has the shape of a child's jack with knobs at the end of each arm. Additional de Haas-van Alphen data for W has been reported by Girvan,⁹ which lends further support to the general features of the larger pieces of the Lomer model. The size-effect experiments by Walsh¹⁰ have pointed out the separation of the electron and hole regions along ΓH , attributed to spin-orbit coupling.

⁶ G. B. Brandt and J. A. Rayne, Phys. Rev. **132**, 1945 (1963).

⁷ D. M. Sparlin and J. A. Marcus, Bull. Am. Phys. Soc. **8**, 258 (1963).

⁸ D. M. Sparlin and J. A. Marcus, Bull. Am. Phys. Soc. **9**, 250 (1964).

⁹ R. F. Girvan, M.S. thesis, Iowa State University, 1964 (unpublished).

¹⁰ W. M. Walsh, Jr., and C. C. Grimes, Phys. Rev. Letters **13**, 523 (1964).

* Contribution No. 1674. Work was performed in the Ames Laboratory of the U. S. Atomic Energy Commission.

¹ W. M. Lomer, Proc. Phys. Soc. (London) **80**, 489 (1962).

² J. H. Wood, Phys. Rev. **126**, 517 (1962).

³ M. Asdente and J. Friedel, Phys. Rev. **124**, 384 (1961).

⁴ M. F. Manning and M. I. Chodorow, Phys. Rev. **56**, 787 (1939)

⁵ W. M. Lomer, Proc. Phys. Soc. (London) **84**, 327 (1964).